An attempt to validate the ultra-accelerated microbar and the concrete performance test with the degree of AAR-induced damage observed in concrete structures

ARTICLE *in* CEMENT AND CONCRETE RESEARCH · JULY 2013

Impact Factor: 3.85 · DOI: 10.1016/j.cemconres.2013.03.014

2 AUTHORS:

Andreas Leemann
Empa - Swiss Federal Laboratories for Mate…
46 PUBLICATIONS **622** CITATIONS
SEE PROFILE

Christine Merz
ungricht merz GmbH
4 PUBLICATIONS **5** CITATIONS
SEE PROFILE

A. Leemann, C. Merz, An attempt to validate the ultra-accelerated microbar and the concrete performance test with the degree of AAR-induced damage observed in concrete structures, Cement and Concrete Research 49 (2013) 29–37, http://dx.doi.org/10.1016/j.cemconres.2013.03.014

An attempt to validate the ultra-accelerated microbar and the concrete performance test with the degree of AAR-induced damage observed in concrete structures

Andreas Leemann, Empa, Swiss Federal Laboratories for Material Science and Technology, Duebendorf, Switzerland
Christine Merz, Holcim (Schweiz) AG, Würenlingen, Switzerland

Abstract

There is little knowledge about the relation between AAR-induced damage observed in structures and the expansion potential obtained with accelerated tests. In this study, aggregates used in structures damaged by AAR were tested with the microbar test (MBT / AFNOR XP 18-594) and the concrete performance test (CPT / AFNOR P18-454). After the tests, the samples were examined using optical and scanning electron microscopy. Based on the results, the significance of the microbar test has to be examined very critically. The agreement of measured expansion, reacted rock types and the composition of the reaction products between the on-site concrete and the reproduced concrete subjected to the CPT clearly indicates that the reaction mechanisms in the structure and in the concrete performance test are comparable. As such, the concrete performance test seems to be an appropriate tool to test the potential reactivity of specific concrete mixtures.

Keywords: alkali aggregate reaction, microbar test, concrete performance test, validation

1 Introduction

The concrete market demands short test durations as it has to be possible to adapt mix designs within a relatively short time frame. This makes it possible to control concrete production and to adjust a mix design, if does not meet the demanded properties. Accordingly, acceleration of the alkali-aggregate reaction is achieved by adding alkalis and by elevating relative humidity and temperature during the tests [eg. 1-5]. The increase in relative humidity ensures the availability of sufficient moisture for AAR to proceed [6]. The increase in temperature has two effects. On one side, the solubility of SiO_2 increases with temperature [7,8]. On the other side, an elevated temperature during the hydration of ordinary Portland cement leads to an increased pH in the

pore solution [9]. Because dissolution rate and solubility of SiO_2 increases with pH [7,10,11], SiO_2 dissolution is further increased. As a result, the increase of alkali content and temperature may cause a reaction of aggregates in a particular accelerated test that are non-reactive in another test. Not surprisingly, the correlation between different test methods can be unsatisfactory [12-15]. A comparison between the reaction products of two accelerated mortar tests (at 38 °C and 100 % RH /at 80 °C in 1M NaOH) and a concrete prism test (at 38 °C, 100 % RH) showed that they are of comparable morphology and chemistry in spite of different alkali levels and temperatures employed [16]. Even more important than the comparability of different accelerated tests is the correlation between laboratory tests and the behaviour of on-site concrete [17]. The transferability of the results obtained with different accelerated test methods may be compromised by differences in the reaction mechanisms. However, expansion is usually the only determined parameter and no data about leached alkalis or changes in the microstructure are usually collected, even if such studies would clearly benefit from an extension of the experimental program in this direction [18-19]. As such, the reason for the frequently poor agreement between the results of different accelerated test methods and the behaviour of on-site concrete often remains obscure. Therefore, a validation of the expansion obtained in different accelerated tests with the degree of damage observed in concrete structures is mandatory.

The starting point of this study was an investigation of different structures in Switzerland damaged by AAR. These structures were selected to cover different geological settings. All structures exhibit damages due to AAR, except one structure which was selected as a reference for an undamaged on-site concrete. The age of the investigated structures ranges from 25 to 40 years. Cores with a diameter of 50 and 100 mm were taken using the same procedure for all structures; a strongly damaged and a weakly damaged area were selected based on a visual inspection. Based on the mechanical properties of the concrete, its porosity and thin section analysis, cement content and water-to-cement ratio (w/c) were estimated (Table 1). The grain size distribution of the aggregates was assessed visually on the concrete cores by comparing the cores with cores of concrete with a known grain size distribution. Since documents from the construction phase were only partially available, the origin of the cement is not known in one case (structure MS). Moreover, some of the cement plants that delivered the cement for the structures are not in operation any more. In such a case cement with a similar composition was chosen. All structures were built using ordinary Portland cement (CEM I according to EN 197-1). The Na_2O-equivalent in the Swiss cements CEM I has no significant variation and ranges from 0.6 to 1.0 mass-%. As all quarries delivering the aggregates for the structures are still in

operation, there was no problem to use aggregates from the same source as used in the specific on-site concrete.

In a first step, the potential reactivity of different groups consisting of similar rock types was determined with the ultra-accelerated microbar test (MBT / AFNOR XP18-594) to assess the influence of aggregate mineralogy on expansion. Then the microbar expansion of aggregates from the quarries that were used to produce the concrete of the damaged structures was measured and compared with the degree of quartz dissolution determined with scanning electron microscopy. These aggregates were additionally used to re-produce the concrete of the damaged structures. Its expansion potential was analysed with the concrete performance test (CPT (AFNOR P18-454) at 60 °C. The expansion of the reproduced concrete is expected to be above the limit value, leading to a classification as potentially reactive. Furthermore, the expansion resulting in the CPT is compared with the crack width observed in the structures. In a complementing approach, the reaction frequency of specific rock types present in the aggregates is determined in the concrete of the structures and in the laboratory concrete by optical microscopy. The composition of the reaction products determined with EDX analysis in both laboratory and on-site concrete is also compared.

2 Materials and methods

2.1 Materials and mixture proportions

Aggregates

The aggregates are named with an abbreviation of the location where they were quarried; the reactive aggregates MA, ME, UR, MS, ME, VI and GU as the reference for a non-reactive aggregate (Table 1). For the MBT two aggregates were added, WE as it is known to be non-reactive in the CPT and in structures, and aggregate SG as it is strongly reactive in the CPT and in structures. Additionally, aggregates consisting of only one rock type were prepared for the MBT [1]. Some of them were separated from aggregates consisting of different rock types, others originate from quarries consisting of a single rock type.

Aggregates MA, MAI, UR, GU, MS, ME and VI were used to produce and test concrete according to AFNOR P 18-454 [3]. All concrete mixtures were produced with CEM I according to EN 197-1 (Table 2). Cements of different plants were used because the aim was to reproduce concrete in structures showing AAR induced damages [20]. Therefore, each combination of cement and aggregate corresponds to a specific mixture used in a specific structure. One series of concrete had a cement content of 300 kg/m^3, the other a cement content of 400 kg/m^3 to cover

the usual range of cement content in on-site concrete and to account for likely variations in the cement content during concrete production. The alkali content of the total amount of cement used in the concrete was increased by 25% as prescribed by AFNOR P18-454 by adding NaOH to the mixing water.

2.2 Methods for assessment and analysis

The areas in the structures showing the highest and lowest degree of damage were selected for crack measurements. Widths of the cracks present on the surface of the concrete structures were determined according to [21] using a magnifier with scale (resolution: 0.05 mm). A square with a side length of 1 m was drawn on the concrete surface. Crack width was measured along two sides of the square and the two diagonals. A crack-index was calculated as width of crack per measured length. The crack width does not take into account the expansion taking place before the cracking occurred. Moreover, there are additional factors like curing conditions and shrinkage that can affect the width of surface cracks. However, the crack widths measured in strongly damaged parts of AAR-affected structures are regarded as meaningful values to characterise concrete expansion [22,23] and were therefore used in the comparison with CPT expansions.

The petrography of the aggregates was determined according to Swiss standard SN 670'115 [24] on the fraction 8/16 mm. The term “quartz-bearing limestone” was used for limestone containing detritic quartz.

The potential reactivity of the aggregates was measured with the MBT [1]. In this test, the expansion of microbars is used to classify aggregates as non-reactive or potentially reactive. First, the aggregates were crushed and sieved to a grain size fraction of 16-63 μm and afterwards, microbars (10 × 10 × 40 mm) with a ratio of cement to aggregate of 2, 5 and 10 were produced. The Na_2O-equivalent of the cement was increased to 1.5 % by adding NaOH. The curing included a vapour treatment above boiling water for four hours and a treatment in a 10 % KOH solution at 150 °C for six hours. The highest mean expansion of the microbars with different cement to aggregate ratios was used to classify the aggregate. An aggregate is classified as potentially reactive when the expansion is ≥ 0.11 %. The MBT shows a good correlation to the NBRI test [2,25].

The potential alkali-aggregate reactivity of the concrete was determined with the CPT [3]. This method was designed to test job-site concrete mixtures. Three prisms (70 × 70 × 282 mm^3) were produced, stored at 20 °C and demoulded after 24 h. Afterwards, they were stored at 60 °C and 100% relative humidity for 20 weeks. Every four weeks, their mass and length was measured at

20 °C (cooling period of 24 h). When the expansion after 20 weeks exceeds 0.02% (mix designs with CEM I), the concrete is classified as unsuitable for use in structures according to AFNOR FDP 18-456 [26]. This test method is very similar to RILEM AAR 4, which has been assessed in an extensive study conducted by a number of international laboratories as a very consistent method that clearly identifies alkali aggregate reactivity [27]. With 0.03% the expansion limit of this test is higher than in the CPT.

For the investigation with SEM, samples from the MBT and CPT were cut along their length axis. Then, the microbars and selected parts of the concrete prisms were grinded with only little pressure applied, dried in an oven at 50 °C for three days, impregnated with epoxy resin, polished and carbon coated. About 1.0 mm of the surface was removed by polishing to remove artefacts (microcracks, cavities created by weakly attached particles) caused by cutting the samples before impregnation. Images were made with an environmental scanning electron microscope (ESEM-FEG XL30). The samples were studied in the high-vacuum mode (2.0-6.0 × 10^{-6} Torr) with an accelerating voltage of 15 kV and a beam current of 180-200 mA. Point analysis was conducted with energy dispersive X-ray spectroscopy (EDX) to identify the chemical composition of aggregates or minerals in aggregates. An EDAX 194 UTW detector, a Philips digital controller, and Genesis Spectrum Software (Version 4.6.1) with ZAF corrections were used. Based on the grey scale values, aggregates and voids within the aggregates were segmented with a software developed in Matlab (Figure 1). This software contains different filters facilitating image analysis. The voids were attributed to dissolved quartz. Occasionally, dissolution features were observed on feldspars. The feldspar dissolution was not accounted for as its extent was minor. Therefore, the total amount of dissolved minerals within an aggregate is referred to as the amount of “dissolved quartz”. In some aggregates like gneiss, it was not possible to segment quartz properly as the grey scale values of the feldspars orthoclase and anorthite are too close to quartz. In such cases, the minerals were identified with EDX point analysis and the quartz content of the particular aggregates was assessed visually. In aggregates like limestone containing detritic quartz, a segmentation of the quartz was easy. 100-150 particles were analysed per aggregate. In the MBT, the reaction products usually extrude the aggregate leaving open voids. Reaction products in aggregates are mostly present as minor residues.

For the microscopy of the on-site concrete, cores from a depth (distance from the concrete surface) > 15 cm were selected. The samples for SEM were prepared in the same way as the samples used in the CPT. Only reaction products in the interior of aggregate particles were analysed, as the reaction products at the edge of the aggregate particles often show considerable

calcium uptake [28]. To exclude an influence of the minerals bordering the reaction products due to the interaction volume of the electron beam, only reaction products in cracks wider than 5 µm were selected for analysis. In fact, in cement hydrates the interaction volume with the chosen acceleration voltage is typically in the range of 1-3 µm [29]. The chemical composition of the reaction products was studied in 6-8 different aggregates summing up to 100-200 point analysed per concrete. Two structures with a broad range of different rock types in the aggregates (MF and VI) and one structure with gneiss aggregate (MB) were chosen for analysis.

The samples of the on-site concrete used for optical microscopy were dried in an oven at 50 °C for three days, impregnated with epoxy resin containing a fluorescent dye and polished before preparing thin sections with a thickness of approximately 20 µm. Using a Zeiss Axiophot they were studied at a magnification of 25 × and 50 × both in transmitted light with crossed polars and in reflected light with a filter enabling the activation of the fluorescent dye. The latter facilitated the identification of cracks. As for the petrography, between 200 and 450 particles with a diameter > 2 mm were identified both in the on-site concrete (area with strong damage) and in the lab concrete (mixtures with 400 kg/m^3 of cement after the CPT). For the determination of the petrography, only particles with a diameter > 2 mm were chosen because of increasing labour with decreasing particle size and increasing uncertainty of the results. After determining the petrography of the particles > 2 mm, the petrography was redone taking into account only reacted particles. Classified as “reacted” were particles containing reaction products in cracks and/or exhibiting cracks running from the particles into the paste. The number-% of reacted particles were normalized to 100 % and the difference to the total aggregates present was calculated (Table 3). Consequently, aggregates reacting frequently result in a positive value and aggregates that do not react or react only rarely in a negative value. This analysis was made for the structures MF, ME and VI. This analysis is suited to identify problematic rock types in aggregates consisting of various rock types. Moreover, it permits a comparison of reacting rock types between the on-site and the lab concrete. The other structures were not suited for such an analysis as the aggregates consisted only of gneiss (structure MS) or because an insufficient number of reacted aggregates was present in the concrete for a representative analysis (structures GU, MA and UR).

3 Results

3.1 Crack measurements on the structures

The crack widths in strongly damaged areas of the structures differ significantly between the different structures. The values are expressed as expansion per meter and year for comparison taking the simplified assumption of a linear expansion over the lifetime of the structures (Table 4). The reference structure for non-reactive concrete has the lowest expansion rate, while structure MS displays the highest values.

3.2 Microbar test (MBT)

The microbar expansion within a specific rock type and between the different rock types shows a significant variation (Figure 2). As an example, mean expansion of gneiss is relatively low, but the values vary from 0.03 to 0.28 %. The range of expansion measured with sandstone and siliceous limestone is similar. Siliceous limestone displays the highest mean value followed by quartzite, sandstone, gneiss and limestone. No significant expansion is expected from the limestone as it contains quartz only as impurities (< 2 mass-%).

The amount of dissolved quartz in aggregates seems to increase along with the increasing quartz content of the aggregates, if the two gneiss aggregates (SG and MS) are not taken into account (Figure 3). In relation to their quartz content, quartz dissolution in the two gneiss aggregates is relatively low. However, microbar expansion does not correlate well with the amount of dissolved quartz: it varies from 0.04-0.25 % at 4-6 % dissolved quartz (Figure 4).

3.3 Concrete performance test

At a cement content of 300 kg/m^3, four of seven concrete mixtures already exceed the limit value of 0.020 % (Figure 5a). Aggregate MS leads to a particular high expansion. At a cement content of 400 kg/m^3 all concrete mixtures, except the one with aggregate GU used as non-reactive reference, reach expansions above 0.020 % (Figure 5b). The increase in cement content increases the expansion of all concrete mixtures. However, the relative increase going along with the increase in cement content is specific for each aggregate and is especially pronounced in the concrete produced with aggregate VI.

3.4 Optical microscopy

In structure MF, quartz-bearing limestone and rhyolite show the most frequent reaction, while sandstone reacts only rarely (Figures 6a-c). The same behaviour is observed in the lab concrete, with gneiss being the exception. Gneiss shows a low tendency to react in the structures but a high one in the lab concrete.

Siliceous limestone and quartz-bearing limestone are the rock types reacting most frequently in structure ME. At the other end of the scale is limestone; as it does not contain SiO_2 other than as impurities (< 2 mass-%), it cannot expand significantly. The lab concrete reflects the situation in the on-site concrete: generally, the same rock types show a high and a low frequency to react. However, the values of the lab concrete are considerably higher compared to the on-site concrete.

Again, siliceous limestone and quartz-bearing limestone are the frequently reacting rock types in structure VI. Gneiss and limestone react only rarely or do not react. The values for the lab concrete are similar.

Apart of structure VI, the number of reacted aggregates is generally higher in the on-site compared to the lab concrete (Table 5).

3.5 EDX analysis

The differences in the chemical composition of the reaction products are relatively small (Table 6, Figure 7). Their silicon content ranges from 62.3 to 75.2 mol-%, calcium content from 12.5 to 19.4 mol-% and alkali content from 11.8 to 19.5 mol-%. The highest Ca/Si-ratio is present in lab concrete MF (0.31) and the lowest in lab concrete MB (0.17). Na/K-ratio displays a range of 0.29 to 0.47 in the on-site concrete and 0.13 to 0.39 in the lab concrete.

Assessed qualitatively, the reaction products in cracks within the aggregates are significantly more common in the on-site concrete than in the lab concrete. On the other hand, gaps at the interface between paste and aggregate and in voids in the paste close to the interface are more often filled with reaction products in the lab concrete than in the on-site concrete.

4 Discussion

The significant variations in microbar expansion within a specific rock type could be attributed to the heterogeneity in regard to texture of the aggregates (presence of cleavage/layering, grain size and spatial distribution of quartz) and differences in quartz properties. Such differences can be expected as aggregates of the same rock type originate from different geological and tectonic units (so-called “nappes”). In particular, the mechanical stress conditions and temperature in the geological history of the rocks can have a significant influence on quartz reactivity; they govern the frequency of defects in the lattice structure of the mineral and with it the proneness to hydroxide attack [eg. 30-32]. Based on this situation, it is obvious that even if petrography may be able to identify some potentially reactive aggregates, it is not able to give an assessment about

the degree of reactivity. An assessment of reactivity is often based on experience rather than on the identification of quartz features indicating high reactivity.

The relation between quartz content of the aggregates and dissolved quartz in the MBT is only weak. The variation in the results, especially in regard to gneiss, indicate that specific quartz properties as discussed above and aggregate texture have an influence on the extent of quartz dissolution.

The correlation between dissolved quartz and microbar expansion is poor (Figure 4) clearly indicating that the amount of dissolved quartz, and with it the amount of reaction products formed, is not the governing parameter for expansion. In fact, the potential of the reaction products to take up water by either osmosis or capillary suction is influenced by their Ca/Si-ratio [e.g. 33-35]. Moreover, in order to generate stress and strain, the reaction products need a certain viscosity that seems to be dependent on their composition [36,37]. The composition of the reaction products may be influenced by the availability of dissolved calcium that could depend on the texture of the aggregates, the permeability of the aggregates and the distance of the reacting sites to $Ca(OH)_2$ in the cement paste. The reason for the poor correlation is, however, not entirely clear.

The correlation between microbar and CPT expansions is poor (Figure 8). The studied aggregates and concrete mixtures even seem to indicate that a high expansion in the MBT decreases the probability for high expansions in the CPT. For these reason, the meaningfulness of results obtained with ultra-accelerated test methods in general and of the MBT in particular has to be examined critically. The amount of dissolved quartz in the MBT is significantly higher than in the CPT [19]. Moreover, quartz dissolution in ultra-accelerates tests seems to be governed by both the amount of quartz present in the aggregate and its specific characteristics (Figure 3). However, in the CPT and in concrete structures with the same or similar aggregates as tested with the MBT in this study, the expansion is mainly caused by the frequently reacting quartz-bearing limestone and siliceous limestone (Figures 6a-c). As shown in [20], there are aggregates that are classified as non-reactive by the MBT, but cause an expansion above the limit value in the CPT and cause AAR-induced damages in structures.

Reproducing the on-site concrete of damaged structures and subjecting these concrete mixtures to the CPT mostly leads to expansions above the limit value. This is an indication that the CPT is able to assess if a specific concrete mixture is potentially reactive or not. Moreover, expansions in the CPT and expansion rates based on crack width measurements on the structures show the same trend (Figure 9). Obviously, the CPT can give an approximation about the degree of expansion that can occur in structures. Of course such a comparison can only show a reasonable

fit when the AAR in the structure has already reached a well advanced stage. Despite trying to reproduce the on-site concrete as close as possible, some differences in composition could most likely not be prevented. However, it is obvious that the variations and changes in the last decades of both petrography of aggregates from the same quarry and of cement properties do not have a significant influence on the results. The increase in expansion caused by increasing the cement content from 300 to 400 kg/m^3 clearly shows that quartz dissolution, formation of the reaction products and subsequent expansion are not correlated in a linear way. Although, the concrete of structure GU used as reference for undamaged concrete shows little expansion, more concrete mixtures of this kind are needed to prove that the CPT cannot give false positives. However, the experience in the Swiss middle land clearly confirms that concrete identified as non-reactive in the CPT does not lead to damages on structures [20].

The temperature increase in the lab test (60° C) to accelerate AAR does not lead to a reaction of rock types that are not reacting in the structure. This is clearly indicated by the agreement of the pattern of rock types with frequent or rare reaction between on-site and lab concrete. This is a further indication that the AAR in the structure is well reflected in the CPT. However, differences have to be pointed out as well. Firstly, the number of aggregates reacting in the CPT is in some cases significantly lower than in the structure. One reason could be the test duration of 20 weeks, which is not sufficient for a number of aggregates to generate enough pressure to crack. Chemical analyses of the cores (acid- and water-soluble alkalis) did not indicate a significant leaching of alkalis which might have explained the different behaviours in any case [20]. Secondly, the qualitatively assessed differences in the local occurrence of reaction products can be explained with the differences in the temperature. The gelation process accelerates at high temperatures, but the viscosity of silica gel is decreasing with increasing temperature [38]. As a result, the extrusion of reaction products from the aggregates into the paste (with causing little or no cracking), is more frequent in the lab concrete.

In regard to the ratio between silicon, calcium and the sum of potassium and sodium, the reaction products are very similar, despite the differences in exposure and age. This indicates that the reaction mechanisms are comparable as well. The Ca/Si-ratio of the reaction products defines their ability to take up water and swell [33-35] indicating similar properties in this aspect. The variations in the Na/K-ratio are in a similar range and are likely caused by the alkalis available in the pore solution [39] and possible some alkali release by reacting minerals [40,41]. In general, the composition of the reaction products correlates with the one reported in literature [eg. 42,43].

5 Conclusions

The concrete properties and the crack formation of structures damaged by AAR were analysed. In the next step, the potential reactivity of aggregates used in these structures was determined with the MBT. Then the concrete of the structures was reproduced with the same aggregates and subjected to the CPT. The expansion measured on the structures and in the accelerated tests was compared and complemented with microstructural and chemical analysis to build a validation chain.

Measuring microbar expansions of different aggregates, including several ones consisting of only one rock type, and analysing the extent of quartz dissolution in the aggregates during the MBT with electron microscopy and image analysis leads to the following conclusion:

- There is a wide variation in microbar expansion of the same rock type originating from different sources.
- The amount of dissolved quartz seems to depend on the total quartz content of the aggregates. But the properties of the quartz present seem to have a strong influence as well, as indicated by gneiss aggregates showing relatively little quartz dissolution.
- The amount of dissolved quartz shows a poor correlation with microbar expansion.

Comparing the expansions determined with the MBT and the CPT show the limitations of the former:

- There is no correlation between microbar expansion and expansion in the CPT. Even the use of aggregates classified as non-reactive in the MBT can result in concrete expansion exceeding the limit value, so called false positives.
- Ultra-accelerated expansion tests like the MBT have to be examined very critically.

Reproducing the concrete of damaged structures, testing it with the CPT and analysing it with microscopy allows a validation of the accelerated test:

- The majority of the lab concrete mixtures exceeds the limit value for expansion at a cement content of 300 kg/m^3 (Na_2O-equvalent: 2.9-3.4 kg/m^3), while all concrete

mixtures except the non-reactive reference exceed it at a cement content of 400 kg/m^3 (Na_2O-equvalent: 3.9-4.5 kg/m^3).

- Expansion rates determined with crack measurements on structures in advanced state of AAR and expansion in the CPT show a good correlation.
- The same rock types react frequently (above average) respectively rarely (below average) in on-site and lab concrete.
- The chemical composition of the reaction products is very similar in both on-site and lab concrete.

Obviously, non-reactive and potentially reactive concrete mixtures can be distinguished with the CPT. Furthermore, the determined expansion can give an indication about the degree of expansion possible in the structure. As such the CPT is an important tool to develop mix designs for non-reactive concrete and to prevent future damages.

6 Acknowledgement

The authors would like to thank the federal road authorities (ASTRA) for the financial support of the project (AGB 2005/023, AGB 2006/03) and P. Lura for reviewing the manuscript.

7 REFERENCES

[1] AFNOR XP 18-594, Méthodes d'essai de reactivité aux alcalis. Association Française de Normalisation, Paris, 2004.

[2] SABS 1245, Potential reactivity of aggregates with alkalis (accelerated mortar prism method), South African Bureau of Standards, South Africa, 1994.

[3] AFNOR P18-454, Réactivité d'une formule de béton vis-à-vis de l'alcali-réaction (essaie de performance), Association Française de Normalisation, Paris, 2004.

[4] ASTM C 1260-07, Standard test method for potential alkali reactivity of aggregates (mortar-bar method), Annual book of ASTM standards, 2007.

[5] ASTM C 227-10, Standard Test Method for Potential Alkali Reactivity of Cement-Aggregate Combinations (Mortar Bar Method) Annual book of ASTM standards, 2010.

[6] H. Olafson, The effect of relative humidity and temperature on alkali expansion of mortar bars, in: Concrete alkali aggregate reactions, Noyes publications, Far Ridge, NJ, 1986, pp. 461-465.

[7] P.M. Dove, The dissolution kinetics of quartz in sodium chloride solutions at 25° to 300 °C, American Journal of Science 294 (1994) 665–712.
[8] J.P. Icenhower, P.M. Dove, The dissolution kinetics of amorphous silica into sodium chloride solutions: effects of temperature and ionic strength, Geochimica and Cosmochimica Acta 64 (2000) 4193-4203.
[9] B. Lothenbach, F. Winnefeld, C. Alder, E. Wieland, P. Lunk, Effect of temperature on the pore solution, microstructure and hydration products of Portland cement pastes, Cement and Concrete Research 37 (2007) 483-491.
[10] G.B. Alexander, W.M. Heston, R.K. Iler, The solubility of amorphous silica in water, The Journal of Physical Chemistry 58 (1954) 453–455.
[11] J.J. Mazer, J.V. Walther, Dissolution kinetics of silica glass as a function of pH between 40 and 85 °C, Journal of Non-Crystalline Solids 170 (1994) 32-45.
[12] S. Lane, Comparison of results from C 441 and C 1293 with implications for establishing criteria for ASR-resistant concrete, Cement, Concrete and Aggregates 21 (1999) 149-156.
[13] L. Sanchez, S.C. Kuperman, P. Helene, Y. Kihara, Trials to correlate the accelerated mortar test, the standard and the accelerated concrete prism tests, in: M.A.T.M. Broeckmans, B.J. Wigum (Eds.), Proceedings of the 13th ICAAR, Trondheim, Norway, 2008, pp. 1154-1165.
[14] A. Shayan, A, Xu, H. Morris, Comparative study of the concrete prism test (CPT 60°C) and other accelerated tests, in: M.A.T.M. Broeckmans, B.J. Wigum (Eds.), Proceedings of the 13th ICAAR, Trondheim, Norway, 2008, pp. 412-421.
[15] S.U. Einarsdóttir, B.J. Wigum, Alkali-aggregate reaction in Iceland - new test methods, in: M.A.T.M. Broeckmans, B.J. Wigum (Eds.), Proceedings of the 13th ICAAR, Trondheim, Norway, 2008, pp. 340-349.
[16] A. Shayan, M. Quick, Microstructure and composition of AAR products in conventional standard and new accelerated testing, in: K. Okada, S. Nishibayashi, M. Kawamura (Eds.), Proceedings of the 8th ICAAR, Kyoto, Japan, 1989, pp. 475-482.
[17] A. Leemann, J.G. Hammerschlag, C. Thalmann, Inconsistencies between different accelerated test methods used to assess alkali-aggregate reactivity, in: M.A.T.M. Broeckmans, B.J. Wigum (Eds.), Proceedings of the 13th ICAAR, Trondheim, Norway, 2008, pp. 944-953.
[18] M. Thomas, B. Fournier, K. Folliard, J. Ideker, M. Shehata, Test methods for evaluating preventive measures for controlling expansion due to alkali–silica reaction in concrete, Cement and Concrete Research 36 (2006) 1842-1856.

[19] M. Ben Haha, E. Gallucci, A. Guidoum, A, K.L. Scrivener, Relation of expansion due to alkali silica reaction to the degree of reaction measured by SEM image analysis, Cement and Concrete Research 37 (2007) 1206-1214.
[20] C. Merz, A. Leemann, Validierung der AAR-Prüfungen für Neubau und Instandsetzung. ASTRA-Bericht. AGB 2005/023 und AGB 2006/003, Bern, 2012.
[21] LCPC. Détermination de l'indice de fissuration d'un parement de béton, Méthode d'essai LPC 47, 1997.
[22] B. Godart, B. Mahut, P. Fasseu, M. Michel, The guide for aiding to the management of structures damaged by concrete expansion in France, in: M. Tang, M.Deng, M (Eds), Proceedings of the 12th ICAAR, Bejing, China, 2004, 1219-1228.
[23] D. Vézina, D. Bouchard, Concrete highway structures showing signs of ASR distress: monitoring program at the Ministère des Transports du Québec, in: B. Fournier, (Ed), Marc-André Bérubé Symposium on Alkali-Aggregate Reactivity in Concrete, Montréal, Canada, 2006, pp. 413-422.
[24] SN 670'115, Gesteinskörnungen: qualitative und quantitative Mineralogie und Petrographie. Swiss Standard, VSS Zürich, 2005.
[25] J.G. Hammerschlag, P. Zgraggen, Beurteilung der Alkali-Zuschlag-Reaktion der Zuschläge und einzelner Betonrezepturenfür die Alptransit Tunnelprojekte Gotthard und Lötschberg. TFB-Bericht, Projekt 998055, Ref. 05.001/2, 2000.
[26] AFNOR FD P18-456, Réactivité d'une formule de béton vis-à-vis de l'alcali réaction, Association Française de Normalisation, Paris, 2004.
[27] P. Nixon, S. Lane, Experience from testing of the alkali reactivity of European aggregates according to several concrete prism test methods, Partner report 3.3 (SBF52 A06021), SINTEF, Trondheim, Norway, 2006.
[28] T. Katayama, ASR gel in concrete subject to freeze-thaw cycles - comparison between laboratory and field concretes from Newfoundland, Canada, in: M.A.T.M. Broeckmans, B.J. Wigum (Eds.), Proceedings of the 13th ICAAR, Trondheim, Norway, 2008, pp. 174-183.
[29] H.S. Wong, N.R. Buenfeld, Monte Carlo simulation of electron-solid interactions in cement-based materials, Cement and Concrete Research 36 (2006) 1076–82.
[30] P.J.M. Monteiro, K. Shomglin, H.R. Wenk, N.P. Hasparyk, Effect of aggregate deformation on alkali-silica reaction, ACI Materials Journal 98 (2001) 179-83.
[31] M.A.T.M. Broekmans, Structural properties of quartz and their potential role for ASR, Materials Characterization 53 (2004) 129-140.

[32] F. Locati, S. Marfil, E. Baldo, Effect of ductile deformation of quartz-bearing rocks on the alkali-silica reaction, Engineering Geology 116 (2010) 117-128.
[33] W. Wieker, C. Hubert, D. Heidemann, R. Ebert, Alkali–aggregate reaction- a problem of the insufficient fundamental knowledge of its chemical base, in: M. Cohen, S. Mindess, J. Skalny (Eds), Proceedings of the Sidney Diamond Symposium on Materials Science and Engineering of Concrete and Cementious based Composites. Materials Science of Concrete, American Ceramic Society, Westerville, OH, 1998, pp. 395-408.
[34] T. Mansfeld, Das Quellverhalten von Alkalisilikatgelen unter Beachtung ihrer Zusammensetzung (Expansion behaviour of alkali silicate gels considering their composition), Doctoral Thesis, Bauhaus-Universität Weimar, Germany, 2008.
[35] A. Leemann, G. Le Saout, F. Winnefeld, D. Rentsch, B. Lothenbach, Alkali-silica reaction: the influence of calcium on silica dissolution and the formation of reaction products, Journal of the American Ceramic Society 94 (2011) 1243–1249.
[36] H. Krogh, Examination of Synthetic Alkali–Silica Gels, in: Symposium on Alkali-Aggregate Reaction, Icelandic Building Research Institute, Reykjavik, Iceland, 1975, 133-163.
[37] R.K. Iller, The chemistry of silica, Wiley, New York, 1979.
[38] A. Amiri, G. Øye, J. Sjöblom, Temperature and pressure effects on stability and gelation properties of silica suspensions, Colloids and Surfaces A: Physicochemical and Engineering Aspects 378 (2011) 14-21.
[39] A. Leemann, B. Lothenbach, The influence of potassium–sodium ratio in cement on concrete expansion due to alkali-aggregate reaction, Cement and Concrete Research 38 (2008) 1162-1168.
[40] D. Constantiner, S. Diamond, Alkali release from feldspars into pore solutions, Cement and Concrete Research 33 (2003) 549-554.
[41] A. Leemann, L. Holzer, Alkali-aggregate reaction - identifying reactive silicates in complex aggregates by ESEM observation of dissolution features, Cement and Concrete Composites 27 (2005) 796–801.
[42] N. Thaulow, U.H. Jakobson, B. Clark, Composition of alkali silica gel and ettringite in concrete railroad ties: SEM-EDX and X-ray diffraction analysis, Cement and Concrete Research 26 (1996) 309-318.
[43] T. Knudsen, N. Taulow, Quantitative microanalyses of alkali-silica gel in concrete, Cement and Concrete Research 5 (1975) 443-454.

region and county	location, type of structure, year of construction	cement content [kg/m^3]	w/c	aggregate $Ø_{max}$ [mm]	label of aggregate and structure	present rock types (in order of decreasing amount)
Midland, Solothurn	Wangen, viaduct, 1977	325-350	0.45 - 0.50	32	GU	sandstone, quartzite, gneiss, siliceous limestone, limestone
Jura, Neuchâtel	Thielle, supporting wall, 1970/77	350-400	0.43 - 0.45	22	MA	limestone, limestone with detritic quartz, gneiss, sandstone, siliceous limestone, quartzite
Alps, Wallis	Mattsand, dam, 1963	400	0.45 - 0.50	60	MS	gneiss
Prealps, Vaud	Bornisses, supporting wall, 1967-68	400	0.45 - 0.50	32	VI	limestone with detritic quartz, siliceous limestone, gneiss, quartz, limestone, schist
Prealps, Uri	Rorbach, bridge, 1982-83	350-400	0.45 - 0.50	20	UR	gneiss, siliceous limestone, sandstone, schist, limestone with detritic quartz, quartzite
Prealps, St. Gallen	Mels, viaduct, 1969	300-350	0.45	20	MF	limestone with detritic quartz, sandstone, gneiss, quartzite, schist, granophyr
Prealps, Vaud	Mur 10, supporting wall, 1980	400	0.43 - 0.45	32	ME	limestone with detritic quartz, siliceous limestone, limestone, sandstone, gneiss, quartzite, silex

Table 1: Location, type and abbreviated name of the investigated structures with a simplified petrography of the aggregates (n.a. = not analysed, aggregate Ømax = maximum grain size used in structure).

concrete	cement content [kg/m^3]	Na_2O-equ of cement [mass-%]	Na_2O-equ of concrete including NaOH addition [kg/m^3]	w/c
GU	300 / 400	0.79	2.96 / 3.95	0.45
MAI	300 / 400	0.78	2.93 / 3.90	0.45
UR	300 / 400	0.80	3.00 / 4.00	0.50
MA	300 / 400	0.90	3.38 / 4.50	0.45
MS	300 / 400	0.77	2.89 / 3.85	0.50
ME	300 / 400	0.83	3.11 / 4.15	0.45
VI	300 / 400	0.83	3.11 / 4.15	0.45

Table 2: Concrete mixtures used for the CPT.

column	A	B	C	D
rock types	total aggregates [number-%]	reacted aggregates [number-%]	reacted aggregates (column B) normalized to 100%) [number-%]	difference between reacted aggregates (column C) and total aggregates (column A [number-%]
gneiss	7.2	2.5	9.4	2.2
quartzite	4.0	0.7	2.7	-1.3
sandstone	5.8	1.1	4	-1.8
siliceous limestone	28.9	8.7	32	3.1
quartz-bearing limestone	46.7	14.1	52	5.3
limestone	7.2	0	0	-7.2
sum	100.0	27.2	100.0	-

Table 3: Petrography of aggregate ME (on-site concrete); total aggregates present, the reacted aggregates (as number-% and normalized to 100 %) and their relative difference.

structure	GU	MF	UR	MA	MS	ME	VI
crack index [mm/m]	0.33	1.44	1.08	2.1	4.7	0.60	2.5
expansion rate [mm/m·y]	0.010	0.035	0.040	0.060	0.100	0.020	0.060

Table 4: Expansion rate of strongly damaged areas of the structures based on crack width measurements.

structure	reacted aggregate particles [number-%]	
	on-site	CPT
MF	30	11
UR	36	<3
ME	27	15
VI	34	35

Table 5: Amount of reacted aggregate particles in the on-site and the lab concrete.

structure	concrete	Si [mol-%]	Ca [mol-%]	Na [mol-%]	K [mol-%]	Ca/Si	Na/K
MF	on-site concrete	63.3	17.2	6.1	13.4	0.27	0.47
	lab concrete	62.3	19.4	6.6	10.3	0.31	0.39
UR	on-site concrete	68.7	15.0	3.7	12.6	0.21	0.29
	lab concrete	68.1	17.0	1.8	13.1	0.25	0.13
MB	on-site concrete	72.9	15.3	2.7	9.1	0.21	0.30
	lab concrete	75.2	12.5	2.6	9.7	0.17	0.27

Table 6: Chemical composition of the reaction products analyzed within aggregates of on-site and lab concrete (after the CPT).

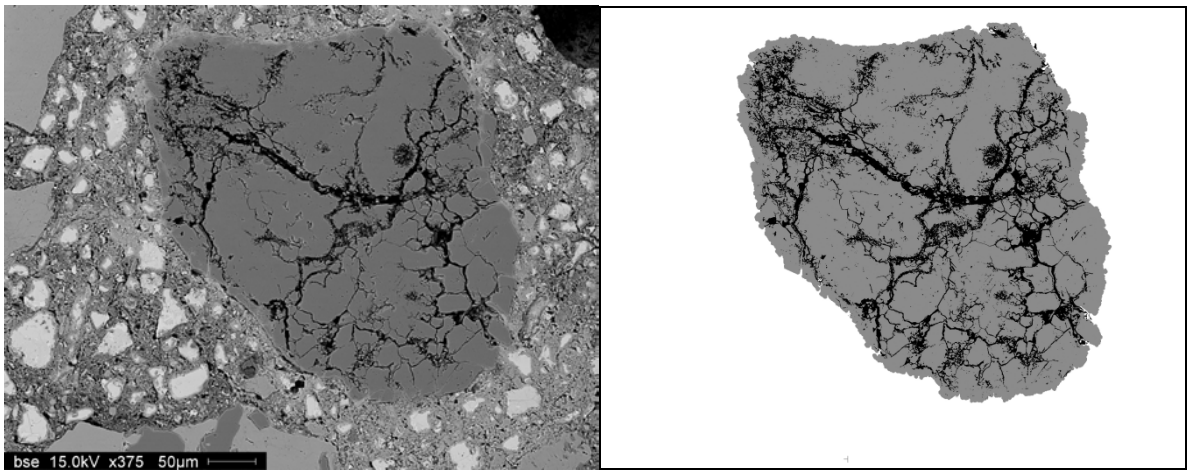

Figure 1: Quartzite aggregate displaying dissolved quartz as black voids (left side) and a segmentation of this image (grey = aggregate, black = dissolved quartz, content of dissolved quartz = 18%, right side).

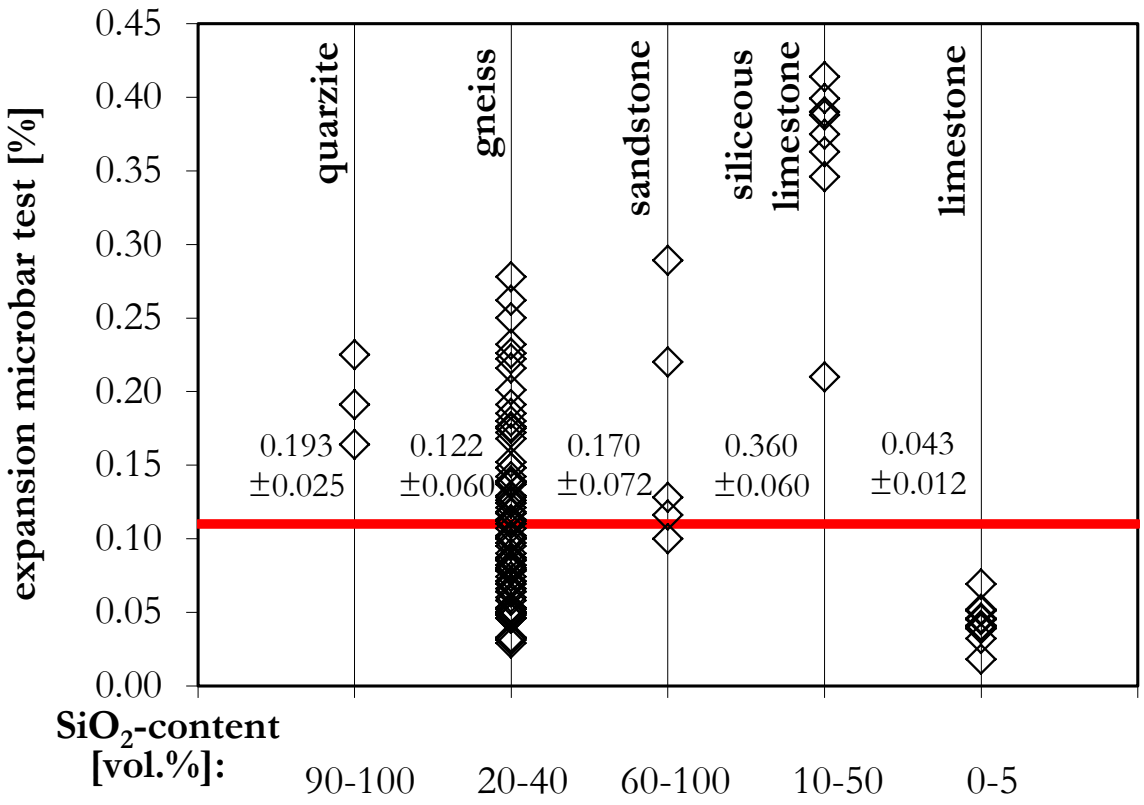

Figure 2: Microbar expansion of specific rock types (101 aggregates: 3 quartzites, 74 gneisses, 5 sandstones, 8 siliceous limestones, 11 limestones / numbers on the left side of the symbols: mean value and standard deviation). The horizontal line represents the limit value for the MBT.

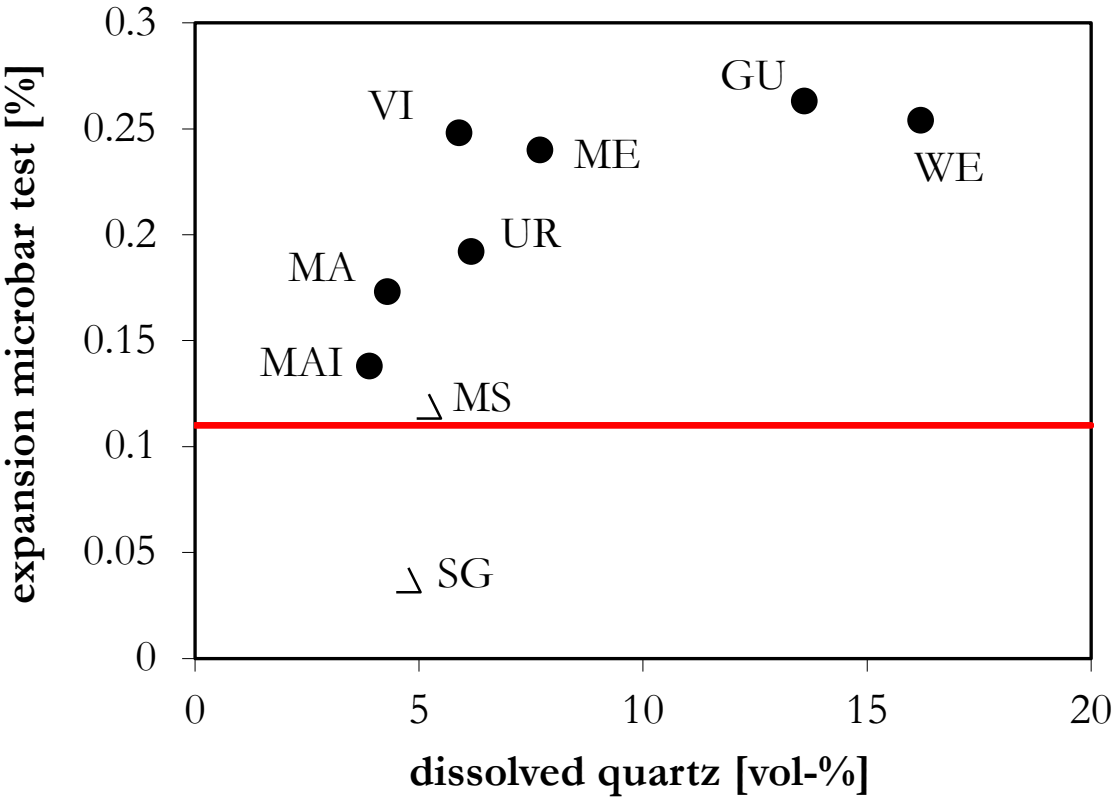

Figure 4: Expansion in the MBT as a function of the amount of dissolved quartz within the aggregates (circle: aggregate consisting of various rock types, triangle: aggregate mainly consisting of gneiss). The line represents the limit value for the MBT.

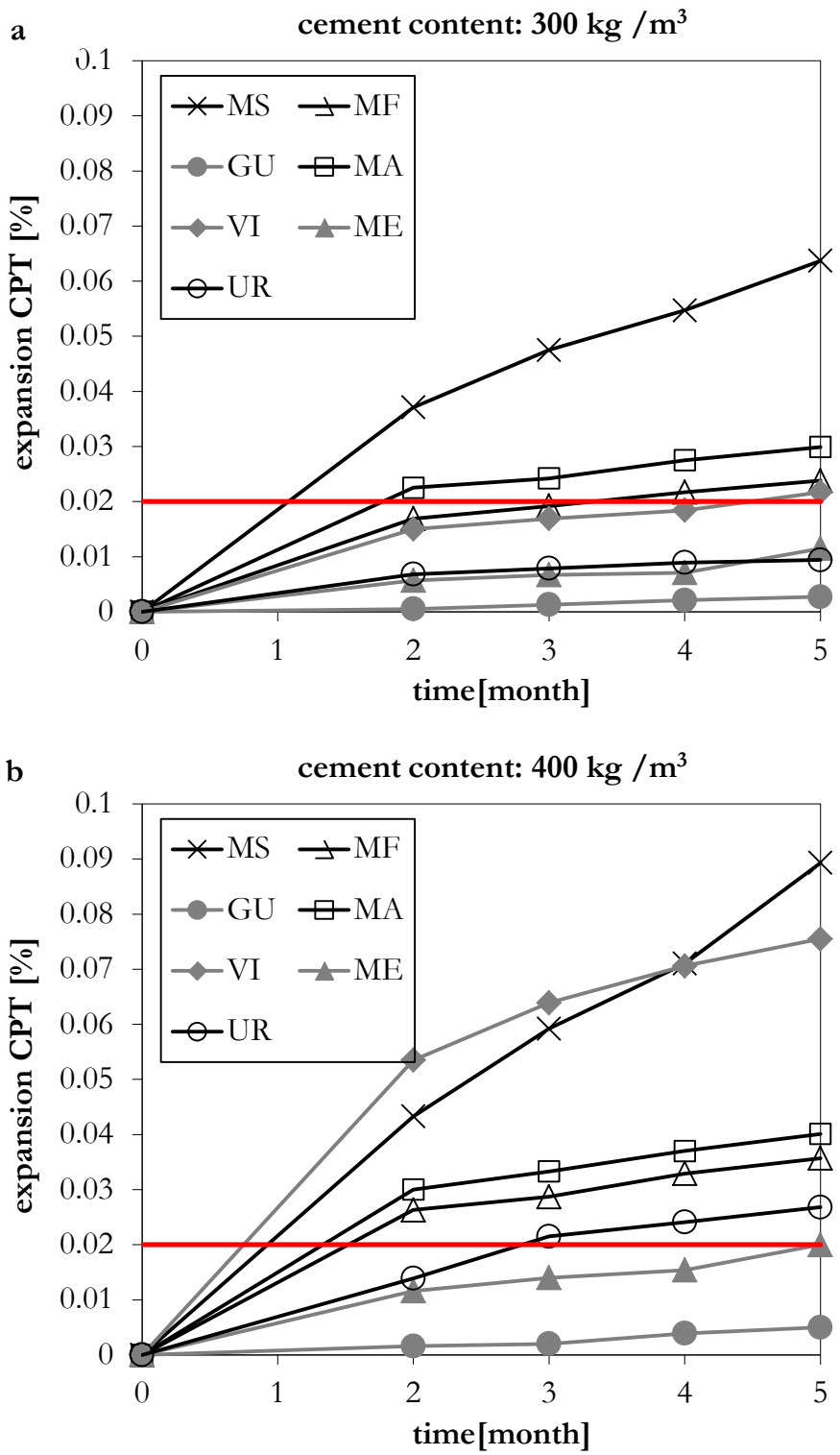

Figures 5a and 5b: Expansion of the lab concrete using a cement content of 300 and 400 kg/m^3.

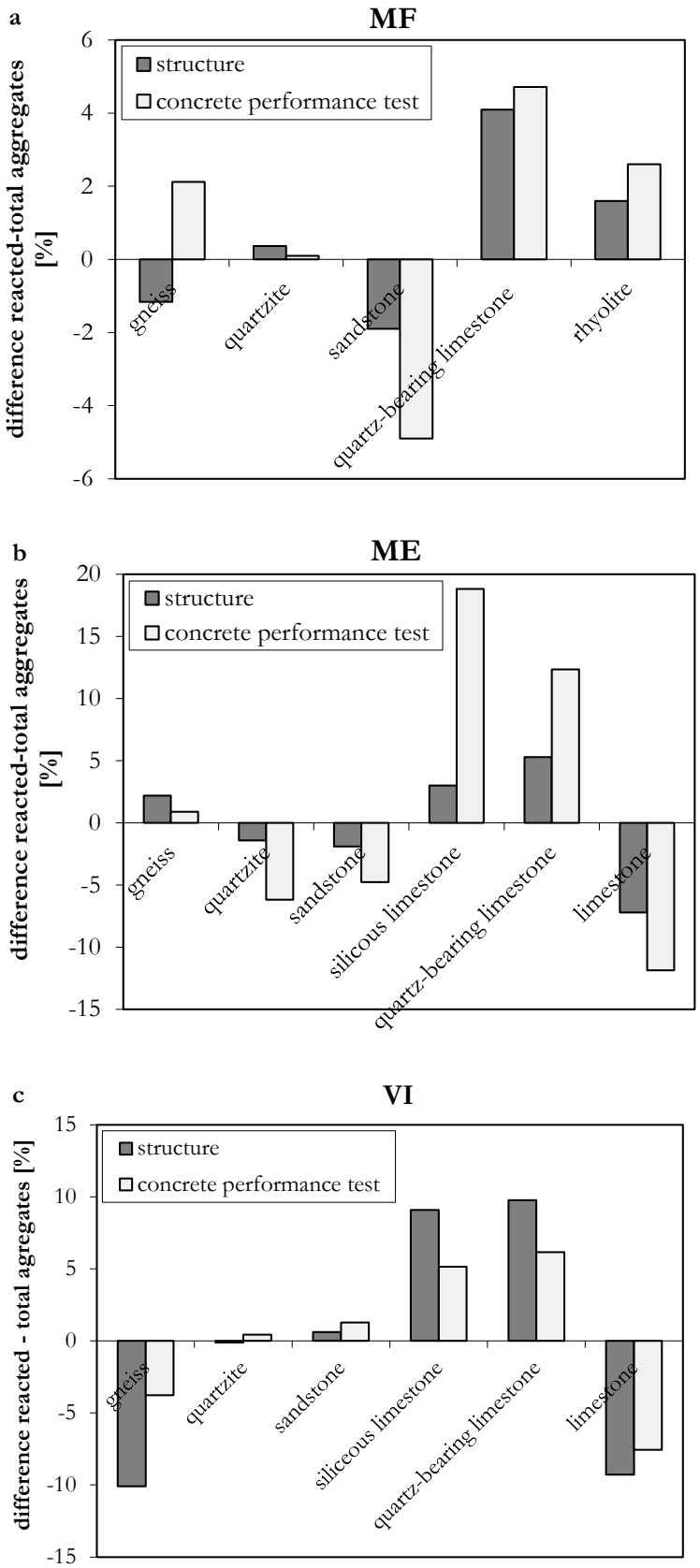

Figures 6a-c: Relative difference between reacted aggregates (normalized to 100 %) and total aggregates present of rock types showing above (positive values) or below (negative values) average frequency of reaction in on-site concrete and in lab concrete after the CPT (structures MF, ME and VI).

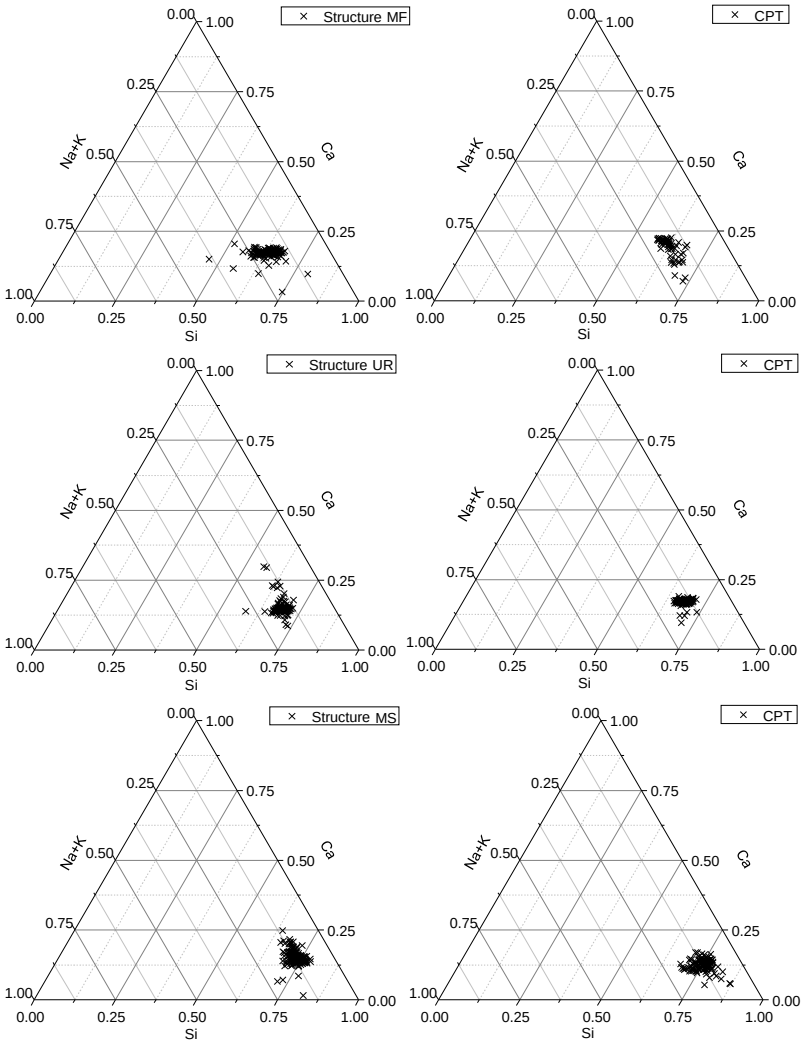

Figure 7: Composition of the reaction products the in on-site concrete and the in lab concrete after the CPT (structures MF, UR and MS).

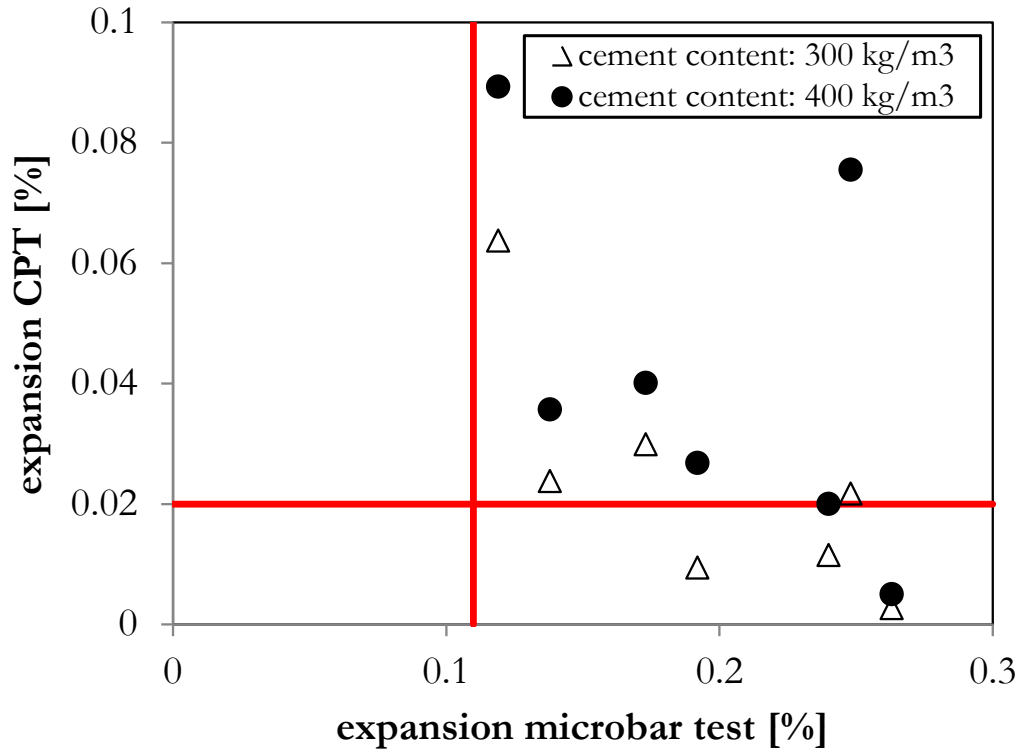

Figure 8: Expansion in the CPT as a function of the expansion in the MBT.

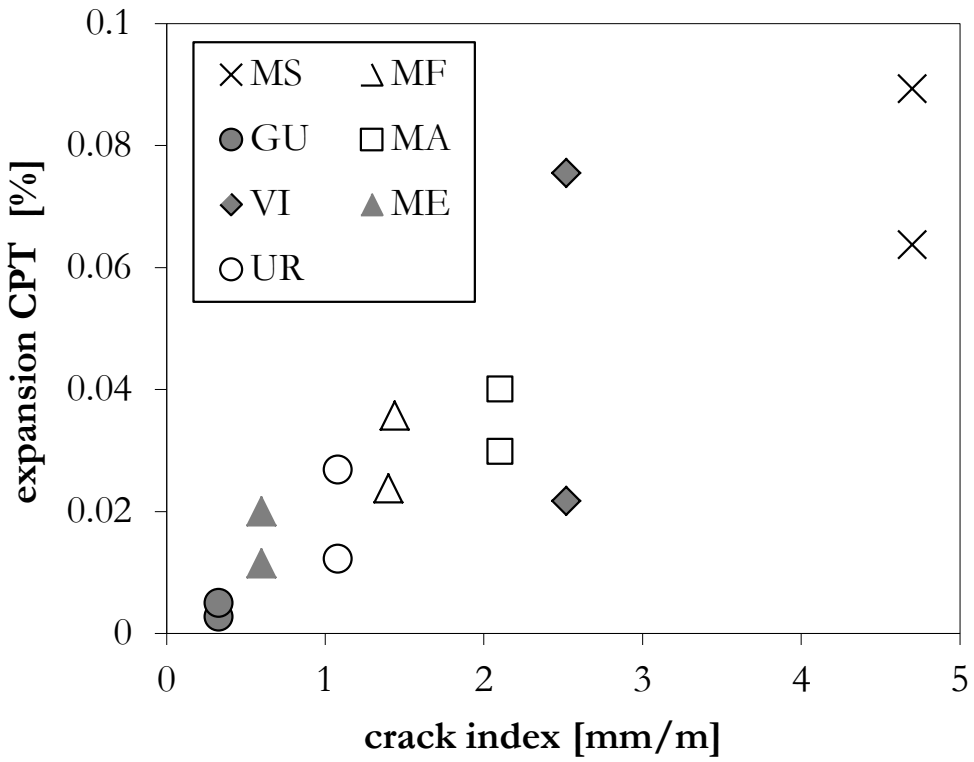

Figure 9: Expansion in the CPT (cement content of 300 and 400 kg/m^3) as a function of the crack-index determined on the investigated structures.